



ELSEVIER

Journal of Archaeological Science xx (2005) 1–10

 Journal of
**Archaeological
 SCIENCE**
<http://www.elsevier.com/locate/jas>

The emerald and gold necklace from Oplontis, Vesuvian Area, Naples, Italy

Carlo Aurisicchio ^{a,*}, Alessia Corami ^b, Sylvana Ehrman ^c,
 Giorgio Graziani ^b, Stella Nunziante Cesaro ^d

^a *Istituto di Geoscienze e Georisorse, Consiglio Nazionale delle Ricerche (IGG-CNR Sezione di Roma),*

c/o Dipartimento Scienze della Terra (DST), Università di Roma "La Sapienza", p.le A. Moro 5, 00185 Roma, Italy

^b *Dipartimento di Scienze della Terra (DST), Università di Roma "La Sapienza", p.le A. Moro 5, 00185 Roma, Italy*

^c *Scientific Methodologies Applied To Cultural Heritage (SMATCH), Largo U. Bartolomei 5, 00136 Roma, Italy*

^d *Istituto per lo Studio dei materiali nanostrutturati (ISMN-CNR), c/o DC, Università di Roma "La Sapienza",
 p.le A. Moro 5, 00185 Roma, Italy*

Received 9 February 2005; received in revised form 30 August 2005; accepted 18 October 2005

Abstract

The present study refers to the characterization of an emerald and gold necklace, dating from the first century AD, found in Oplontis (Torre Annunziata, Naples, Italy), using non-destructive methodologies such as EPMA and microFTIR. Reference samples, from mines known to be active in the Roman Imperial period, were collected and analyzed using the same techniques. Experimental data were also statistically treated in order to classify the emeralds' mines. The comparison of archaeological and reference data allowed to hypothesize, with high probability, an Egyptian origin for the Oplontis emeralds – even if the Habachtal mine cannot be definitively excluded.

© 2005 Elsevier Ltd. All rights reserved.

Keywords: Archaeological jewels; Emerald; Beryl; Gemmology; Microanalysis; Infrared spectroscopy; Oplontis

1. Introduction

A society's degree of development can be determined through careful study of its artefacts. Information so gleaned can provide a comprehensive picture of daily life, including the cultural level reached in various social classes. Studies of objects fashioned from precious metals, ornamental stones, gemstones and technologies employed in creating and decorating jewellery provide a wealth of information on Imperial Rome's use of raw materials, its artistic tastes and decorative values, and how jewellery was used as an indicator of social status [2].

The origin of gemstones from archaeological finds has always been a particular challenge for researchers [4,12,25].

Scientists and archaeologists have combined efforts in an attempt to determine the possible commercial exchange routes that brought goods to Rome. Of all gemstones, according to Pliny the Elder [22], emeralds were the most popular. In his *Naturalis Historia* (Book 37, 62) he wrote, "no colour is more attractive than their (green) colour. Furthermore, it is the only gem that satisfies without tiring the eyes."

This study presents the results of gemmological and geochemical analyses carried out on emeralds that were part of a gold necklace found during excavations undertaken on a Roman villa in Oplontis, which coincides with the modern city of Torre Annunziata.

2. History

During systematic excavations that started in 1964 two suburban villas buried by the eruption of Mount Vesuvius in AD 79 [23] came to light. According to archaeologists the first one, sumptuous in size and decoration, belonged to Poppea, wife of

* Corresponding author.

E-mail addresses: carlo.aurisicchio@uniroma1.it (C. Aurisicchio), sjhrman@libero.it (S. Ehrman), giorgio.graziani@uniroma1.it (G. Graziani), stelluccia.nunziante@ismn.cnr.it (S.N. Cesaro).

the Emperor Nero. The second one, more modest but still quite large, was probably oriented toward farming and trade [11].

A signet ring found on the premises of this villa bears the name “Lucius Crassus Tertius”, possibly the owner. Numerous amphorae for storing wine, pomegranate and other goods were found. In Room 10 of the villa, 54 skeletons were gathered. Many of them were wearing or holding gold or silver coins, as well as jewellery items, in a desperate and futile attempt to flee to safety with precious belongings. Judging by the quantity of objects and coins next to it, skeleton no. 27 was probably a person of importance. Nineteen prismatic beads of emerald, the subject of this study, and 24 golden beads likely belonging to a necklace whose thread was missing, were among these objects (Fig. 1). The necklace is now part of the collection (inventory no. 3412a) of the Soprintendenza di Pompei (Naples).

3. Description and gemmology

The necklace is 58 cm long and is made of an alternate succession of 24 oval plain gold beads (1.3×0.7 mm average)



Fig. 1. Ensemble of the jewels found near skeleton no. 27 in the villa of Poppea (Oplontis, Naples, Italy). For size, see Section 3.

and 19 hexagonal prisms of emerald crystals; 14 of them are shown in Fig. 2. The missing clasp was probably a loop and hook, as was the style in Imperial Rome. This piece is unique for its peculiar look, showing a succession of emeralds mounted on a gold chain. If the pieces found represent the entire necklace, then it is probable that there was a series of gold pieces toward the clasp. The chromatic succession of yellow and deep green of gold and emerald and the simplicity of the design give the piece a rare and stunning elegance (A. D’Ambrosio, pers. comm., 2001).

Optical and physical gemmological tests were performed on the 19 hexagonal emerald prisms, using standard equipment. Their average dimensions fell between 9.8×8.9 mm (minimum) and 14.7×9.8 mm (maximum). All had been drilled lengthwise to form the necklace. To the unaided eye, all crystals appeared greasy and transparent to semitransparent/opaque under natural light and bluish to deep green in colour, with etching, scratches and accidental breakage. The determined average density was 2.64 and pleochroism showed yellowish green for the ordinary ray and light blue green for the extraordinary ray. Some surfaces of the crystals were sufficiently polished to permit spot reading: 1.57 and refractive indices, as determined with a Duplex II refractometer, were $n_{\omega} = 1.581$ and $n_{\varepsilon} = 1.588$, with a birefringence of 0.007. High values of refractive indices suggest high octahedral substitutions for Al in the emeralds structure (see Table 1). Microscopic observation showed characteristic fine tubules, two-phase liquid/gas inclusions, mica flakes and limonite solid inclusions and cavities parallel to the optic axes of the prismatic crystals. Absorption spectra exhibited a typical emerald trend, with slight changes in the strength of the main observed lines: 683.5 and 680.6 nm.

All specimens examined gave gemmological parameters in a narrow range, suggesting that all are likely of the same origin.

4. Analytical tests

Through study of their inclusions, gemmological tests can provide data that help determine gemstone origins, even when results obtained from samples coming from different sources overlap and preclude definitive identification of provenance. To narrow a range of possible origins to a single source requires that further analyses be performed. Electron Probe Micro Analysis (EPMA) equipped with Wavelength Dispersive Spectrometers (WDS) and microFTIR (Fourier Transform InfraRed) Spectroscopy, among other non-destructive analytical methods, were used to determine the chemical composition and structure of the emeralds. More recently developed methodologies, as described in the literature, are also available. Proton induced X- and gamma-ray emissions (PIXE/PIGE) seem to give promising results [7,9] even if they require software improvements for use in data processing. Ion-microprobe analysis of $^{18}\text{O}/^{16}\text{O}$ isotopic ratio, which is related to the crystallization environment, can differentiate emeralds originating in various deposits [12–14]. As an invasive technique, it cannot always be used even if the damage is very limited.



Fig. 2. Overall view of the stunning gold and emerald necklace found in Poppea's villa in Oplontis, Naples, Italy and details of single gold beads and emeralds. For size, see Section 3.

Data collected on the Oplontis gems were compared with results obtained on reference samples of known provenance, such as the Eppler Collection, Italian Museums, private collection, or purchased in laboratories of Idar Oberstein coming from mines known or likely to have been in use during the Roman Empire. According to Pliny the Elder's *Naturalis Historia* (L.XXXVII 65–76), these were presumably the emerald mining localities within the Sikait–Zabara region in the south eastern desert of Egypt [1,3,26], Ekaterinburg and the Urals in Russia, Pakistan, Afghanistan and India¹. Samples from the Habachtal mine (Austria) were also examined. This

¹ Jebel Sikait, Jebel Zabara, Egyptian region of emeralds' mines (Tertium locum Aegyptii habent. Eruuntur circa Copton, oppidum Thebaidis collibus excavatis. Pliny, Nat. Hist. 37, 65); Ethiopia (Ab his Aethiopici laudantur ab Copto dierum itinere, ut auctor est Iuba, XXV, acriter virides, sed non facile puri aut concolores. Pliny, Nat. Hist. 37, 69); Urals (Nobilissimi Scythici, ab ea gente, in qua reperiuntur appellati. Pliny, Nat. Hist. 37, 65); Pakistan; Afghanistan (Proximam laudem habent, sicut et sedem, Bactriani. Pliny, Nat. Hist. 37, 65); India (Eandem multis naturam aut certe similem habere berullii videntur. India eos gignit, raro alibi repositos. Pliny, Nat. Hist. 37, 76).

deposit (not mentioned by Pliny) seems, however, to have been known to the Celts and probably was exploited by the Romans [13,28]. Reference emeralds were also subjected to destructive technique examination, such as X-ray powder diffraction (XRD) and gas chromatography (GC) [6].

4.1. Infrared spectroscopy

Using an IRscope II (Bruker), microFTIR reflectance spectra were recorded in the spectral range 5000–600 cm^{-1} for all 19 emerald prisms, both on pinacoid and prismatic faces. In routine spectra with a resolution of 2 cm^{-1} , 200 scans were accumulated, with a beam diameter of 20 μm .

The spectroscopic behaviour of both pinacoid and prismatic faces was identical for all beads, within the limit of experimental error, suggesting that all the gemstones come from the same mine.

Skeletal bands of emeralds, that is vibrations involving silicon–oxygen, aluminium–oxygen and beryllium–oxygen bonds, lie under 1400 cm^{-1} . Alkali atoms and small molecules, such as carbon dioxide and water, can be located in

Table 1
Average chemical composition (base and prism) of four beads of Oplontis necklace

Oxides wt(%)	Ap ^a	Ab	Bp	Bb	Cp	Cb	Dp	Db
SiO ₂	65.73	65.84	65.72	65.81	65.75	65.81	65.81	65.86
Al ₂ O ₃	13.17	13.30	13.80	13.86	13.86	13.97	13.75	12.96
FeO ^b	1.01	0.70	0.46	0.40	0.44	0.45	0.51	0.93
MnO	0.00	0.01	0.05	0.00	0.00	0.01	0.02	0.05
MgO	2.58	2.60	2.60	2.63	2.61	2.46	2.67	2.63
Cr ₂ O ₃	0.40	0.21	0.35	0.11	0.27	0.25	0.14	0.20
V ₂ O ₅	0.22	0.05	0.08	0.03	0.02	0.03	0.06	0.07
TiO ₂	0.03	0.03	0.00	0.13	0.03	0.02	0.04	0.03
CaO	0.02	0.09	0.02	0.01	0.07	0.08	0.04	0.23
Na ₂ O	1.75	2.02	1.82	1.90	1.81	1.74	1.82	1.93
K ₂ O	0.10	0.13	0.08	0.07	0.12	0.14	0.10	0.11
Cs ₂ O	0.00	0.02	0.01	0.04	0.02	0.04	0.05	0.00
Total	85.00 ^c	85.00	85.00	85.00	85.00	85.00	85.00	85.00

Number of ions on basis of 15 oxygens

Si	6.083	6.089	6.065	6.068	6.066	6.070	6.072	6.100
Al	1.436	1.450	1.501	1.506	1.508	1.519	1.496	1.415
Fe ²⁺	0.078	0.054	0.036	0.031	0.034	0.035	0.039	0.072
Mn	0.000	0.001	0.004	0.000	0.000	0.001	0.001	0.004
Mg	0.355	0.359	0.358	0.362	0.358	0.339	0.367	0.363
Cr	0.029	0.015	0.025	0.008	0.019	0.018	0.010	0.015
V	0.013	0.003	0.005	0.002	0.001	0.002	0.004	0.004
Ti	0.002	0.002	0.000	0.009	0.002	0.002	0.003	0.002
Y tot	1.997	1.884	1.929	1.987	1.923	1.914	1.993	1.874
Ca	0.002	0.009	0.002	0.001	0.007	0.008	0.004	0.023
Na	0.314	0.362	0.326	0.340	0.324	0.312	0.325	0.347
K	0.011	0.015	0.009	0.008	0.015	0.017	0.012	0.013
Cs	0.000	0.001	0.000	0.001	0.001	0.002	0.002	0.000
X tot	0.328	0.387	0.338	0.350	0.346	0.338	0.342	0.383

^a A, B, C, D represent the analyses of the four beads on the base (b) and prism face (p).

^b All the iron has been calculated as FeO.

^c All the analyses have been normalized to 85% because light elements (Li, Be and H) have not been analyzed.

the channels. The asymmetric stretching mode of CO₂ falls in the interval 2400–2300 cm⁻¹, and stretching and bending modes of H₂O absorb in the 3800–3500 and 1750–1500 cm⁻¹ ranges, respectively [24]. Since bands assigned to host molecules are very weak in the case of solid samples, only skeletal bands are discussed below.

The discussion of molecules in the channels will be treated in a paper reporting spectra of the powdered samples diluted in potassium bromide (C. Aurisicchio et al., work in progress). Figs. 3 and 4 collect spectroscopic patterns of the base and prism of one of the beads. These figures also provide comparative data on observed spectroscopic behaviour, with and without polarization, at 0°, 45° and 90° with respect to the C₆ axis.

4.2. Chemical analyses

All of the 19 Oplontis necklace gemstones showed similar gemmological and infrared behaviour. For this reason four were selected, as representative of the whole set, to determine their chemical composition. Analyses were performed using EPMA (Cameca CX 827), equipped with four wavelength

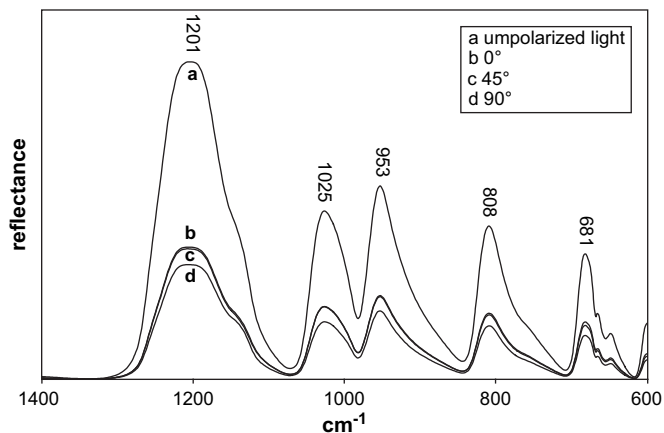


Fig. 3. FTIR spectrum of pinacoid face of one of the beads studied in non-polarized and polarized (0°, 45° and 90°) with respect to C₆ axis.

dispersive spectrometers. Some inclusion-free areas on the pinacoid and prismatic faces were selected for the analyses. All elements were analyzed with an accelerating voltage of 15 kV, a sample current of 30 nA, measured on an andradite mineral standard, and a beam diameter of 3 μm.

This methodology does not allow light element determinations (H, Li, Be, B), whose measurement is possible only by destructive techniques. Be and B content can be determined in microprobe analysis using special analyser crystals not included in the set of Cameca analysing crystals. Na, Mg, Al, Si, K, Ca, Sc, Ti, V, Cr, Mn, Fe, Cs and F were extensively investigated. F, Sc, Ti and Cs, being below detection limits, were not further considered in routine analysis. Water content was not determined. The analytical error was approximately 1% relative for major elements and 5% for minor elements. Detection limits ranged between 0.05 and 0.1 wt%. To compare data, the total for each analysis was normalized to 85 wt%, assuming an average content of 12–13 wt% of BeO and 2–3 wt% of H₂O. In Table 1, two analyses each (pinacoid and prism) are given for the four studied gemstones, which yielded similar

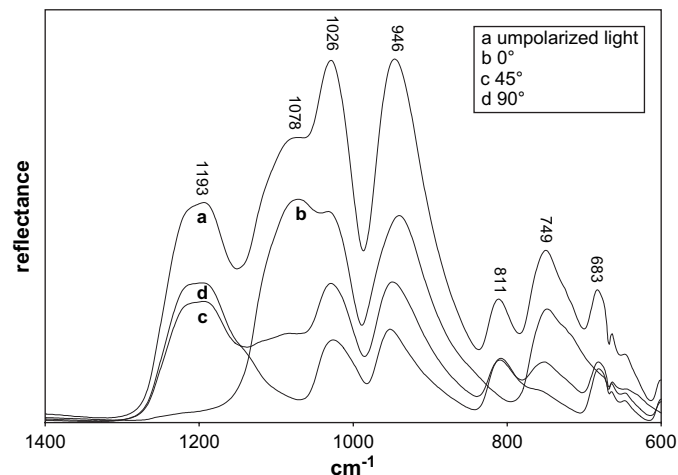


Fig. 4. FTIR spectrum of prismatic face of one of the beads studied in non-polarized and polarized (0°, 45° and 90°) with respect to C₆ axis.

results. Table 2 shows average percentage compositions, the number of analyses for each sample and the standard deviation for historical emerald mine samples. It also shows their formulae calculated on the basis of 15 atoms of oxygen [6].

Because of the homogeneity of the studied emeralds, a single analysis is reported for the Pakistan, Afghanistan and India mines. Two compositions are indicated where samples showed sharp differences, as in the case of the two crystals coming from Russia (likely from different mines) and the Habachtal. Two compositions are also given for the two studied Egyptian mines, even if they appear very close.

Based on chemical data of reference emeralds, statistical processing was used to classify them as to their origin [10]. Data on archaeological emeralds were similarly processed. The obtained trend is treated in Section 5.

5. Discussion

This study of the emeralds from the Oplontis necklace was undertaken with two objectives: to determine their mineralogy and chemical composition and to identify their probable origin.

Gemmological tests and spectroscopic analyses demonstrated the homogeneity of the Oplontis gemstones, suggesting their common origin, but did not suffice as to their provenance.

Chemical analyses, reported in Table 1, show closely similar compositions and support the hypotheses of homogeneity and a common origin of the gems. Any peculiar differences between prismatic and basal faces have been noted. The mineralogical structure, in particular, shows important substitutions in the octahedral site for Al, whereas the tetrahedral site T'' is saturated by Si. Among the major elements the Al content in the emeralds may be considered to be diagnostic of the different geological settings, showing a wide compositional range. However, because the amount of Al in a crystal cannot be related to the bulk composition of the parent mineralizing fluids, a direct link between the Al content and a particular mine of origin cannot be established, and mines having comparable Al contents may have different geological origins.

Mg, Fe²⁺ and Cr, with average values of 0.358, 0.047 and 0.017 apfu (atoms per formulae units), respectively, and minor amounts of V, Ti and Mn, mainly substitute Al in the octahedral site. As a consequence the medium Al content of these gemstones, around 1.479 apfu, can be considered as one of

Table 2
Average chemical compositions and standard deviations of the emeralds from historical mines

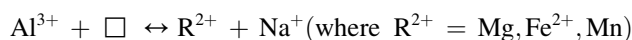
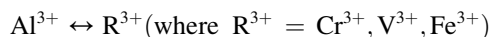
	El Sikait (n = 18)	El Zabara (n = 18)	Habachtal (n = 13)	Habachtal (n = 11)	Ekaterinburg (n = 8)	Urals (n = 11)	Pakistan (n = 30)	Afghanistan (n = 16)	India (n = 9)
SiO ₂	65.94 ± 0.6	65.41 ± 0.31	65.21 ± 0.05	64.82 ± 0.22	65.92 ± 0.26	65.28 ± 0.16	64.92 ± 0.39	66.11 ± 0.72	65.21 ± 0.06
Al ₂ O ₃	13.78 ± 0.12	14.14 ± 0.38	13.65 ± 0.24	15.15 ± 0.27	16.58 ± 0.05	14.71 ± 0.54	13.29 ± 0.34	16.88 ± 0.66	16.27 ± 0.31
FeO ^a	0.50 ± 0.06	0.47 ± 0.02	0.68 ± 0.17	0.33 ± 0.06	0.25 ± 0.03	0.53 ± 0.04	1.33 ± 0.01	0.15 ± 0.01	0.39 ± 0.08
MnO	0.01 ± 0.02	0.01 ± 0.00	0.01 ± 0.00	0.02 ± 0.00	0.01 ± 0.00	0.01 ± 0.00	0.01 ± 0.00	0.03 ± 0.01	0.01 ± 0.01
MgO	2.44 ± 0.15	2.49 ± 0.04	2.62 ± 0.11	2.28 ± 0.04	1.04 ± 0.19	2.34 ± 0.08	2.37 ± 0.13	0.82 ± 0.13	1.20 ± 0.14
Cr ₂ O ₃	0.17 ± 0.01	0.74 ± 0.09	0.70 ± 0.05	0.30 ± 0.02	0.04 ± 0.02	0.50 ± 0.04	1.09 ± 0.03	0.14 ± 0.03	0.35 ± 0.01
V ₂ O ₅	0.08 ± 0.05	0.10 ± 0.00	0.03 ± 0.01	0.05 ± 0.02	0.03 ± 0.02	0.10 ± 0.01	0.08 ± 0.04	0.13 ± 0.04	0.04 ± 0.02
TiO ₂	0.00 ± 0.00	0.00 ± 0.00	0.01 ± 0.00	0.00 ± 0.00	0.01 ± 0.00	0.01 ± 0.00	0.01 ± 0.00	0.01 ± 0.00	0.01 ± 0.00
CaO	0.05 ± 0.01	0.04 ± 0.00	0.01 ± 0.01	0.04 ± 0.01	0.01 ± 0.01	0.03 ± 0.01	0.12 ± 0.06	0.02 ± 0.02	0.03 ± 0.01
Na ₂ O	1.77 ± 0.11	1.52 ± 0.06	2.02 ± 0.12	1.87 ± 0.07	0.95 ± 0.04	1.41 ± 0.04	1.69 ± 0.13	0.68 ± 0.09	1.33 ± 0.06
K ₂ O	0.20 ± 0.04	0.03 ± 0.00	0.02 ± 0.01	0.05 ± 0.04	0.02 ± 0.01	0.04 ± 0.01	0.02 ± 0.01	0.02 ± 0.01	0.07 ± 0.02
CS ₂ O	0.06 ± 0.07	0.05 ± 0.04	0.04 ± 0.01	0.09 ± 0.05	0.11 ± 0.05	0.05 ± 0.02	0.04 ± 0.02	0.02 ± 0.02	0.09 ± 0.02
Total	85.00 ^b	85.00	85.00	85.00	85.00	85.00	85.00	85.00	85.00
Number of ions on basis of 15 oxygens									
Si	6.080	6.006	6.013	5.973	6.025	5.998	5.997	6.022	5.980
Al	1.498	1.531	1.484	1.646	1.790	1.594	1.447	1.813	1.759
Fe ²⁺	0.039	0.036	0.052	0.025	0.019	0.041	0.103	0.011	0.030
Mn	0.001	0.001	0.001	0.002	0.001	0.001	0.001	0.002	0.001
Mg	0.335	0.341	0.360	0.313	0.142	0.320	0.326	0.111	0.164
Cr	0.024	0.102	0.097	0.042	0.005	0.069	0.151	0.019	0.048
V	0.002	0.006	0.002	0.003	0.002	0.006	0.005	0.008	0.002
Ti	0.000	0.000	0.001	0.000	0.001	0.001	0.001	0.000	0.001
Y tot	1.899	2.017	1.997	2.003	1.959	2.029	2.030	1.965	1.985
Ca	0.005	0.004	0.001	0.004	0.001	0.003	0.012	0.002	0.003
Na	0.316	0.278	0.361	0.334	0.168	0.251	0.303	0.120	0.236
K	0.024	0.004	0.002	0.006	0.002	0.005	0.002	0.002	0.008
Cs	0.002	0.002	0.002	0.004	0.004	0.002	0.002	0.001	0.004
X tot	0.347	0.287	0.366	0.347	0.176	0.261	0.318	0.125	0.251

n = Number of analyses considered for each average.

^a All the iron has been calculated as FeO.

^b All the analyses have been normalized to 85%, because light elements (Li, Be and H) have not been analyzed.

the lower values, when compared with those reported in literature [15,21]. The Fe^{2+} content (0.078–0.031 apfu) is variable within relatively wide limits, whereas Mg is homogeneously distributed. Among minor elements substituting Al, Cr and V show some variability. The substitutions of divalent ions for Al inside octahedral sites and Li for Be inside tetrahedral sites unbalance the electric charge, which is restored by Na, Ca, K or Cs entering in the channels formed by the stacking of hexagonal rings of SiO_4 tetrahedra along the c axis. Na (0.324 apfu) is the only alkaline ion hosted in the emerald structure. Substitution mechanisms are:



The known range of beryl compositions can be subdivided into two series, the first with prevailing octahedral substitutions and the second with prevailing tetrahedral substitutions. The two types do not occur together [5].

Considering the diagram of total substitutions in the Al octahedral site plotted against substitutions in the Be tetrahedral site (Fig. 5) [5], where the two beryl series are indicated, it is possible to draw some conclusions about the Oplontis emeralds. Having octahedral substitutions ranging around 0.43 apfu, they fall on the trend of beryl samples showing increasing octahedral substitutions. The tetrahedral substitutions should be very low and, as a consequence, the T' site, usually occupied by Be, should in this case be saturated by this element and the Li content should therefore be negligible. All these inferences confirm their crystallization from an environment rich in Mg, Fe and Cr.

Comparing compositions reported in Table 1 with average compositions of historic mine emeralds (Table 2) helps to suggest the provenance of the Oplontis necklace emeralds. Emeralds from the eight reference mines fall into two groups having a different average Al content. The first one, with Al_2O_3 around 13–14%, MgO 2.42% and FeO 0.57%, comprises samples from the Egyptian emeralds mine region – both El Sikait and El Zabara, Pakistan (Swat Valley), Russia (Urals) and

one of the reported analyses for the Habachtal (Austria). The origin of these mines is mainly determined by tectonic structures, such as thrust faults and shear zones. The circulating fluids, interacting with mafic rocks of volcano-sedimentary series, gave rise to the emeralds mineralization. Emeralds occur in pockets and lenses localized in the contact area between gneissic biotite granite and overlying mica schists (Egyptian and Pakistani deposits) [1,17,18]. Emeralds from Ural mines originate from a metasomatic reaction by interaction of fluid rock pegmatite and mafic rocks, whereas those from the Habachtal are formed by mica-schist protolith and ultramafic rocks interaction [16,20].

The second group, with Al_2O_3 around 15–16%, MgO 1.16% and FeO 0.38%, includes samples from Afghanistan, India, Russia (Ekaterinburg) and the Habachtal. The samples richer in Al, from Afghanistan and India, occur in albite-quartz veins cutting host metamorphosed limestones, phyllites and mica schists. The emeralds are of hydrothermal origin and should be the product of the interaction between volatile-rich melt (forming veins) and host rocks [8,27].

The amount of Na, the most abundant alkali element, ranges from 1.07 to 1.79% in the two mentioned groups, being affected by the different extent of substitutions.

Russian and Habachtal samples show sharp compositional variation (Table 2), which could be ascribed to differences in the crystallization environment (Russia) or to some zoning of the deposit (Habachtal).

The meaningful correlations reported in Fig. 6 between Al (VI) content vs. the sum of other elements occupying the same site (a) and Mg vs. Na (b) support placing the historic mines in the two quoted groups.

Both diagrams show good trends with opposite slopes, even if Fig. 6a allows a better resolution of the mines. The reported values of the Oplontis gemstones plot in the area which groups the El Sikait, Habachtal and Urals samples (Fig. 6a), whereas in the trend Mg vs. Na, they match the values shown by El Sikait, El Zabara and the Habachtal (Fig. 6b). It is worth noting that the Habachtal compositions (as reported above) fall into the same group (see Table 2).

On the basis of vibrational analysis, degenerate bands (E_{1u}) are predicted in spectra of pinacoid faces and non-degenerate bands (A_{2u}) are expected in spectra of prismatic faces [19]. Owing to the birefringence of the crystal, however, the vibrations of the former symmetry class are still present, with low intensity, in spectra of prismatic faces when incoming light is normal to the principal axis (C_6).

As shown in Fig. 3 polarization in fact induces an overall decrease of the spectrum intensity without affecting the spectral position and the relative intensity of the peaks in the basal section, as expected for degenerate modes.

Spectra recorded on the prismatic faces (Fig. 4) are, in contrast, strongly changed by the different polarization angles of the polarized light compared with non-polarized spectra.

Interestingly, two beads out of 19 showed an opposite behaviour in polarized light, indicating that they were cut with their geometric axis normal to the crystallographic C_6 axis, in order to look like natural hexagonal prisms.

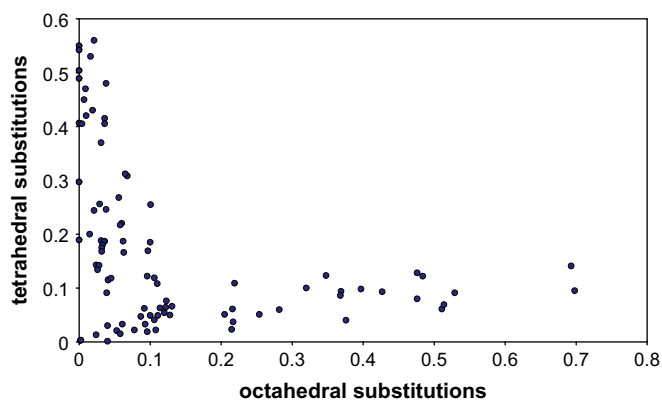


Fig. 5. Total substitutions in the Be tetrahedral site plotted against the total substitutions in the octahedral site. Two distribution series are evident from Ref. [5].

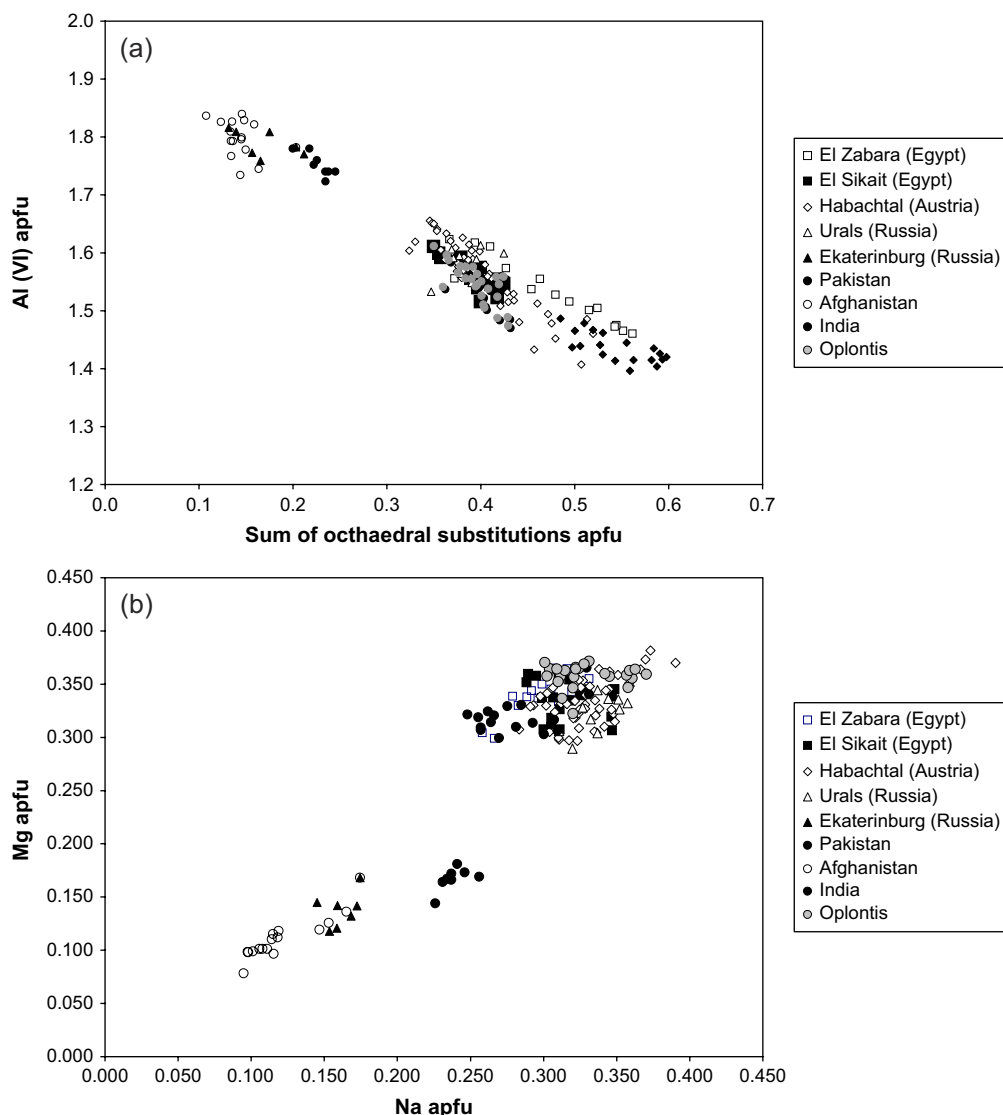


Fig. 6. Correlation Al vs. \sum octahedral substitutions (a) and Mg vs. Na (b) in apfu (atoms per formula unit) showing the area covered by the necklace composition when plotted on reference sample trends.

To surmise the provenance of the Oplontis gemstones, frequency values of their skeletal vibrations were compared with those of stones coming from deposits known to have been mined in early times. Data are limited to spectra of prismatic faces, which yield more information for the number of bands detected and their behaviour under polarization. For the sake of clarity frequency values of reference stone prisms are shown in Fig. 7 and grouped in Table 3, along with those of one of the necklace beads.

As shown in Table 3 and Fig. 7, the position of most of the bands is quite stable, with shifts limited to a range of less than 1% around the average frequency value. In contrast both fundamental broad modes lying at the higher frequency range (around 1220 and 1075 cm^{-1}) present more significant shifts (within 3% around the average value) and seem diagnostic for the different mines, being related to the type and extent of substitutions at the octahedral site. It seems therefore reasonable to

conclude that the mentioned bands, assigned to Si–O stretching, belong to silicon atoms connected – through O-atoms – simultaneously to the rings and to the octahedral site, and are affected by the Al-site substitution. A review of the values reported in Table 3 suggests El Sikait and the Habachtal as the most likely mines of origin for the beads from the necklace.

Furthermore a statistical analysis was developed to discriminate the origin of archaeological emeralds. In this way it was possible to organize the compositions of the different crystals into groups with similar atomic contents (per unity of formula) of analyzed elements and then extract variation patterns between groups. In this case, discriminant analysis shows two variables calculated on the scores of each chemical analysis. Fig. 8 accordingly summarizes the results that divide the emeralds from Oplontis and historic mining regions into four groups. The first one, well defined, contains Pakistani compositions. The second is wider and gathers mines in India,

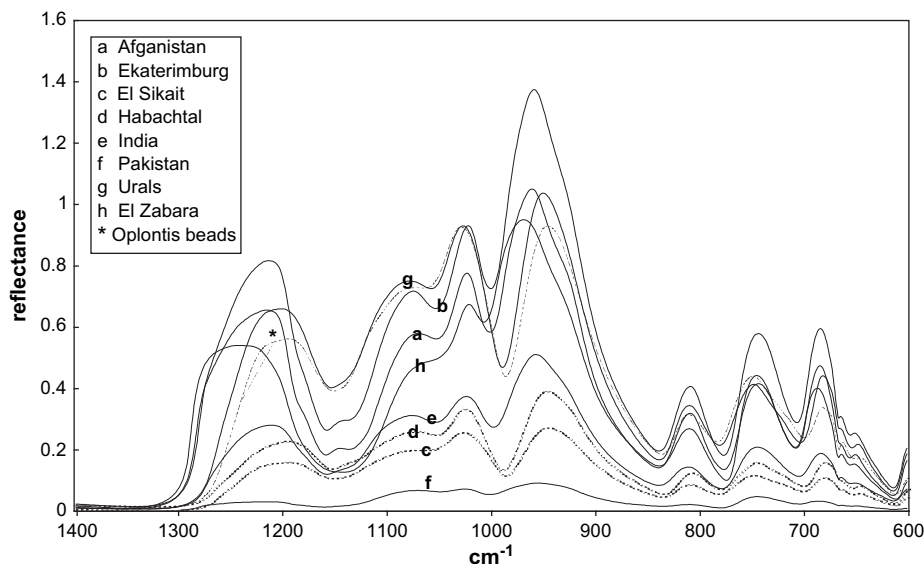


Fig. 7. FTIR spectra of prismatic faces of reference samples in non-polarized light: a – Afghanistan, b – Ekaterinburg (Russia), c – El Sikait (Egypt), d – Habachtal (Austria), e – India, f – Pakistan, g – Urals (Russia), h – El Zabara (Egypt) and *Oplontis necklace. Patterns*, c – and d – are in dotted line because an origin from El Sikait or Habachtal is proposed for the Oplontis gemstones.

Ekaterinburg and Afghanistan. The third and fourth groups, very close to each other, fall along the negative side of the Y-axis and include samples from El Zabara, the Habachtal, the Urals and El Sikait deposits. The Oplontis emeralds lie at the lower border of the third and fourth groups, partly falling in an unknown area of origin and partly overlapping with the composition of emeralds from El Sikait. The unknown area could include the Egyptian mines which we did not characterize for lack of reference samples.

The statistical analysis therefore agrees with the EPMA and FTIR results, suggesting the Egyptian mine of El Sikait as the most probable origin of the Oplontis emeralds.

Gemmological analysis ascertained the presence of mica and limonite inclusions in the Oplontis emeralds. This further supports the hypothesis of an El Sikait, rather than a Habachtal, origin according to the literature [18,29].

6. Conclusions

The Oplontis emeralds were examined using non-destructive and non-invasive techniques to classify them and narrow their origin down to one out of several historic mines. Each

technique suggested a limited number of possible provenances. The gemstones behaved slightly differently when subjected to EPMA measurements: the trend Al(VI) vs. Σ octahedral substituents for Al (Fig. 6a) suggesting a possible El Sikait, Habachtal (composition showing lower Al content, Table 2) or Urals mines provenance, whereas Mg vs. Na (Fig. 6b) suggested similarity to emeralds from El Sikait, El Zabara or the Habachtal. FTIR spectra indicated either El Sikait or Habachtal.

Statistical analysis shows that Oplontis emeralds best match the El Sikait samples, even if some of them fall in an area not covered by reference gemstones.

All reported data and analyses support the hypothesis that the emeralds on the Oplontis necklace were traded to Rome from the El Sikait deposit, one of several famous Egyptian mines, although an Austrian source cannot be excluded, assuming that the mine was active at that time.

Compositional and spectroscopic data suggest both Habachtal and El Sikait as plausible origins for the Oplontis gemstones. However, statistical treatment and gemmological observation of inclusions indicate that the second provenance is more likely.

Table 3
Vibration (cm^{-1}) on prismatic faces of reference and Oplontis emeralds

Afghanistan (Panjshir)	El Sikait (Egypt)	Habachtal (Austria)	India	Pakistan (Swat Valley)	Urals (Russia)	Ekaterinburg (Russia)	El Zabara (Egypt)	Oplontis necklace
1217 ms	1196 ms	1197 ms	1229 ms	1205 ms	1202 ms	1214 ms	1220 ms	1193 ms
1070 m, sh	1080 m, sh	1080 m, sh	1096m, sh	1075 m, sh	1080m, sh	1075 m, sh	1070 m, sh	1078 m, sh
1024 s	1026 s	1025 s	1025 s	1025 s	1027 s	1022 s	1025 s	1026 s
811 mw	810 m	809 m	811 m	809 m	810 m	810 m	810 m	811 mw
744 mw	747 m	746 m	745 m	746 m	749 m	744 m	745 m	749 mw
685 mw	681 m	681 m	650 m	647 m	682 m	685 m	681 m	683 mw

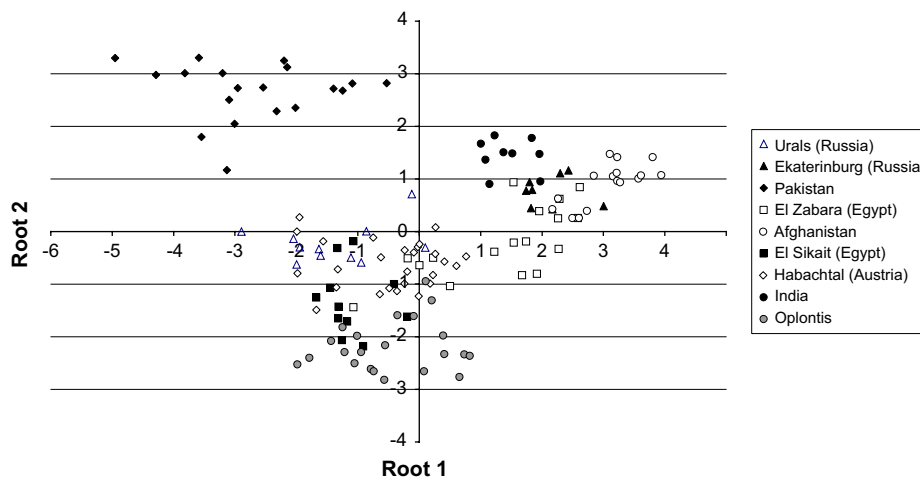


Fig. 8. Distribution of groups obtained by “Discriminant analysis” applied to reference and Oplontis emeralds. Four groups are shown gathering all the compositions considered.

Acknowledgments

This work was supported by the Progetto Finalizzato Beni Culturali (PFBC) of the Italian CNR and developed as a scientific project of the IGG-CNR, Roman Section. The authors are indebted to Dr. A. D’Ambrosio, of the Soprintendenza Archeologica di Pompei, who provided historical background on the studied jewels and placed them at the authors’ disposition. Thanks are also due to D. Manna for photographs of the jewels, to L. Martarelli for his analytical work and to M. Pasini of the Gemmological Laboratory of the Banca di Roma for her help in gemmological analysis. We are indebted to Dr. G. Ciotoli of the Earth Science Department of Rome University “La Sapienza” for his support in statistical analysis. Two anonymous referees commented constructively on an earlier version of this paper.

References

- [1] H.M. Abdalla, F.H. Mohamed, Mineralogical and geochemical investigation of emerald and beryl mineralization, Pan-African belt of Egypt: genetic and exploration aspects, *Journal of African Earth Sciences* 28 (1999) 581–598.
- [2] G.B. Andreozzi, G. Graziani, L. Sagui, Gems from archaeological excavations at Rome (Cripta Balbi), *Zeitschrift der Deutschen Gemmologischen Gesellschaft* 4 (1996) 49–72.
- [3] B.G. Aston, J.A. Harrell, I. Shaw, “Stone” in Ancient Egyptian Materials and Technology, in: P.T. Nicholson, I. Shaw (Eds.), Cambridge University Press, 2000, pp. 5–77.
- [4] C. Aurisicchio, A. Corami, S. Ehrman, D. Ferro, G. Graziani, S. Nunziante Cesaro, A path to identify the origin of archaeological emeralds decorating jewels of Roman Imperial Age, *International Conference Science & Technology in Archaeology & Conservation* 12–18 August 2002, Amman/Petra, Jordan.
- [5] C. Aurisicchio, G. Fioravanti, O. Grubessi, P.F. Zanazzi, Reappraisal of the crystal chemistry of beryl, *American Mineralogist* 73 (1988) 826–837.
- [6] C. Aurisicchio, L. Martarelli, S. Nunziante Cesaro, A. Ciarallo, A. D’Ambrosio, A contribution to the identification of the Oplontis archaeological emeralds origin. *Third International Congress on Science and Technology for the Safeguard of Cultural Heritage in the Mediterranean Basin*, Alcalá de Henares, Spain, 9–14, July 2001.
- [7] C. Aurisicchio, S. Nunziante Cesaro, G. Pappalardo, L. Pappalardo, F.P. Romano, Analisi non distruttiva di un minerale di Berillio mediante i sistemi Pixe-alfa, XRF a microfascio-X del LANDIS/INFN, *Bollettino dell’Accademia Gioenia di Scienze Naturali* 33 (2000) 5–14.
- [8] G.W. Bowersox, A status report on gemstones from Afghanistan, *Gems & Gemology* 1 (1986) 192–204.
- [9] T. Calligaro, J.C. Dran, J.P. Poirat, G. Querré, J. Salomon, J.C. Zwaan, PIXE/PIGE characterization of emeralds using an external micro-beam, *Nuclear Instruments and Method in Physics Research B* 161–163 (2002) 769–774.
- [10] J.K. Galbraith, Lu Jiaqing, Cluster and discriminant analysis on time-series as a research tool, *UTIP Working Paper Number 6*, 1999.
- [11] G. Giubelli, *Oplontis*, Poppea’s Villa, Carcavallo Editore, Naples, Italy, 1995.
- [12] G. Giuliani, M. Chaussidon, H.J. Schubnel, D.H. Piat, C. Rollion-Bard, C. France-Lanord, D. Giard, D. de Narvaez, B. Rondeau, Oxygen isotopes and emerald trade routes since antiquity, *Science* 287 (2000) 631–633.
- [13] G. Giuliani, M. Chaussidon, H. Schubnel, D.H. Piatt, C. Rollion-Bard, C. France-Lanord, D. Giard, D. de Narvaez, B. Rondeau, Historique des gisements d’émeraude et identification des émeraues anciennes (1^{ère} partie), *Revue de Gemmologie A.F.G.* 138/139 (1999) 22–23.
- [14] G. Giuliani, C. France-Lanord, P. Coget, D. Schwarz, F. Notary, A. Cheillez, M. Chaussidon, D. Giard, D. Piat, P. Bariand, Vers une carte d’identité isotopique $^{18}\text{O}/^{16}\text{O}$ des émeraues naturelles et synthétiques, *Revue de Gemmologie A.F.G.* 134/135 (1998) 55–70.
- [15] L.A. Groat, D.D. Marshall, G. Giuliani, D.C. Murphy, S.J. Piercey, J.L. Jambor, J.K. Mortensen, T.S. Ercit, R.A. Gault, D.P. Matthey, D. Schwarz, H. Maluski, M.A. Wise, W.W. Wengzynowski, D.W. Eaton, Mineralogical and geochemical study of the Regal Ridge emerald showing, Southeastern Yukon, *The Canadian Mineralogist* 40 (2002) 1313–1338.
- [16] G. Grundmann, G. Morteani, Emerald mineralization during regional metamorphism: the Habachtal (Austria) and Leydsdorp (Transvaal, South Africa) deposits, *Economic Geology* 84 (1989) 1835–1849.
- [17] E.J. Gubelin, Gemstones of Pakistan: emerald, ruby, and spinel, *Gems & Gemology* 18 (1982) 123–139.
- [18] R.H. Jennings, R.C. Kammerling, A. Kovaltchouk, G.P. Calderon, M.K. El Baz, J.I. Koivula, Emeralds and green beryls of upper Egypt, *Gems & Gemology* 29 (1993) 100–115.
- [19] C.C. Kim, M.I. Bell, D.A. McKeown, Vibrational analysis of beryl ($\text{Be}_3\text{Al}_2\text{Si}_6\text{O}_{18}$) and its constituent ring (Si_6O_{18}), *Physica B* 205 (1995) 193–208 (and refs. therein).

- [20] A.F. Laskovenkov, V.I. Zhernakov, An update on the Ural emerald mines, *Gems & Gemology* 31 (1995) 106–113.
- [21] I. Moroz, I.Z. Eliezeri, Emerald chemistry from different deposits. An electron microprobe study, *Australian Gemmologist* 20 (1998) 64–69.
- [22] Pliny the Elder, *Naturalis Historia: V° Mineralogia e Storia dell'Arte*, Einaudi Editore, 1988, 969 pp.
- [23] Plinio il Giovane, *Lettere ai Familiari (Books I–IX)*, Zanichelli Editore, 1964, 416 pp.
- [24] K. Schmetzer, L. Kiefer, Water in beryl — a contribution to the separability of natural and synthetic emeralds by infrared spectroscopy, *Journal of Gemmology* 22 (1990) 215–223 (and refs. therein).
- [25] D. Schwarz, *Emerald of the World*. ExtraLapis English 2 (2002) pp. 1–100.
- [26] I. Shaw, R. Jameson, J. Bunbury, Emerald mining in Roman and Byzantine Egypt, *Journal of Roman Archaeology* 12 (1999) 203–215.
- [27] J. Sinkakas, *Emeralds and other beryls*, Chilton Book Company, Radnor, Pennsylvania, 1981.
- [28] F. Ward, *Emeralds (Fred Ward Gem Book)*, Paperback, 2002.
- [29] N. Zylberman, *Tableau Synoptique comparative des propriétés gemmologiques des gisements majeurs et des principales synthèses*. (Extraits D.U.G.) in *L'Émeraude*, Association Française de Gemmologie, Paris, 1998 pp. 227–233.